Boundary Signature Matching for Object Recognition

Adnan A. Y. Mustafa
Kuwait University, Department of Mechanical and Industrial Engineering,
P. O. Box 5969 - Safat, Kuwait 13060
Email: symymus@kuc01.kuniv.edu.kw

Abstract

Any object recognition system must address cases when parts of the object are not visible due to occlusion, shadows, ... etc. In this paper we introduce a simple matching method that is based on matching boundary signatures. Boundary signatures are surface feature vectors that reflect the probability of occurrence of a feature of a surface (or an object) boundary. Boundary signatures are an extension to our surface signature formulation which we have presented with good success in our earlier work. We introduce four types of surface boundary signatures; The Curvature Boundary Signature, the Direction Boundary Signature, the Distance Boundary Signature and the Parameter Boundary Signature. These four signatures are constructed based on local and global geometric shape attributes of the boundary. Tests conducted on objects of different shapes have produced excellent results in the absence of occlusion and good results when objects retain at least 70% of their original shapes.

1. Introduction

A major concern with many object matching techniques is that they fail when partial object information is missing. A typical example, is the case of object occlusion where only part of the object is visible to the camera (or vision sensor). Here, the shape of the object and its boundary are no longer similar to its original shape and hence more difficult to match. Such a case usually results in object mismatch and incorrect object hypotheses and hence incorrect recognition. However, depending on how much boundary is missing the object may still retain important features of its boundary that matching using signatures can still produce correct hypotheses. In our previous work, we introduced surface signatures as robust feature descriptors for surface matching [1] [2] [3]. A surface signature is a feature vector that reflects the probability of occurrence of a surface feature on a given surface. Surface signatures are scale and rotation invariant. We showed that by using surface signatures correct identification was possible under partial occlusion and shadows. Previously we employed two types of surface signatures, surface curvature signatures and surface spectral signatures, which statistically represent surface curvature features and surface color features, respectively. In this paper we introduce surface boundary signatures as an extension to our surface signature formulation. Boundary signatures are constructed based on local and global geometric shape attributes of the boundary.

This paper is divided into four sections as follows: section 2 presents a brief review of related work, section 3 introduces the concept of boundary signatures, section 4 describes the matching procedure used, section 5 presents the results of tests conducted and the paper concludes with a discussion of the results in section 6.

2. Related Literature

Shape analysis is divided into two categories, boundary-based shape analysis that analyses the boundary of the shape and interior-based shape analysis that analyses the shapes based on the interior region of the shape. Examples of boundary based shape analysis are Chain (or Freeman) codes, Polygonal Approximations and Shape Signatures. Examples of interior based shaped analysis include region moments methods and Medial Axis Transform (MAT) methods (i.e. skeleton techniques).

The literature on shape analyses methods is vast. In this section we only present a sample of recent papers that are relevant to our work. Hong [4] presented an indexing approach to 2-D object description and recognition that is invariant to rotation, translation, scale, and partial occlusion. The scheme is based on three polygonal approximations of object boundaries where local object structural features (lines and arcs) are extracted. Ozcan and Mohan [5] presented a computationally efficient approach which utilizes genetic algorithms and attributed string representation. Attributed strings were used to

represent the outline features of shapes. Roh and Kweon [6] devised a contour shape signature descriptor to the recognition of planar curved objects in noisy scenes. The descriptor consisting of five-point invariants was used to index a hash table. Nishida [7] proposed an algorithm for matching and recognition of deformed closed contours based on structural features. The contours are described by a few components with rich features. Mokhtarian et. al [8] used the maxima of curvature zero-crossing contours of curvature scale space image as a feature vector to represent the shapes of object boundary contours. Kovalev and Petrou [9] extracted features from co-occurrence matrices containing description and representation of some basic image structures. The extracted features express quantitatively the relative abundance of some elementary structures. For a recent survey on shape analysis techniques the reader is referred to [10].

3. Boundary Signatures

The boundary ($\mathbf{\Omega}$) of any surface (or object) consists of a finite number (N) of an ordered sequence of points (λ) that define the shape of the surface (or object) see Fig. 1,

$$\mathbf{\Omega} = \{ \lambda_i = (x_i, y_i),\ i = 0, \ldots, N-1 \} \tag{1}$$

The following assumptions are made about $\mathbf{\Omega}$,

- $\mathbf{\Omega}$ is closed, i.e. λ_0 follows λ_{N-1}.
- $\mathbf{\Omega}$ has a single point thickness ($\mathbf{\Omega}$ has been thinned)
- $\mathbf{\Omega}$ is traversed in a counter-clockwise sense (the object is to the left)
- $\mathbf{\Omega}$ does not contain any internal holes.

A surface signature is a feature vector that reflects the probability of occurrence of the feature for a given surface. In general, if $\mathbf{S}$ denotes a surface signature of size N, and S_i denotes the ith component of $\mathbf{S}$, then by definition,

$$\sum_{i=0}^{M-1} S_i = 1 \tag{2}$$

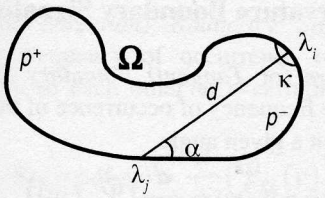

Fig. 1. The feature vectors extracted from the boundary.

where $0 \le S_i \le 1$ and $0 \le i \le M$. We introduce four types of surface shape signatures or surface boundary signatures: the *Angle Boundary Signature* ($\mathbf{S}_{AB}$), the *Curvature Boundary Signature* ($\mathbf{S}_{CB}$), the *Distance Boundary Signature* ($\mathbf{S}_{DB}$) and the *Parameter Boundary Signature* ($\mathbf{S}_{PB}$). These four signatures are constructed based on local and global geometric shape attributes of the boundary ($\mathbf{\Omega}$) as described below. All four signatures $\mathbf{S}_{DB}$, $\mathbf{S}_{AB}$, $\mathbf{S}_{CB}$ and $\mathbf{S}_{PB}$ are rotation, translation and scale invariant.

3.1 The Distance Boundary Signature

The *Distance Boundary Signature* ($\mathbf{S}_{DB}$) represents the frequency of occurrence of the normalized Euclidean distance between two points for a given distance,

$$\mathbf{S}_{DB} = \mathrm{pdf}_{\mathrm{d}}(u) = \frac{d}{du}\left(\tilde{\Psi}_{\mathrm{d}}(u)\right) \tag{3}$$

where $\tilde{\Psi}_{\mathrm{d}}$ denotes the normalized inverse distance function obtained by normalizing the inverse distance function with respect to the maximum inverse distance value,

$$\tilde{\Psi}_d(u) = \frac{\Psi_d(u)}{\max(\Psi_d(u))} \tag{4}$$

where,

$$\Psi_{\mathrm{d}}(u) = f^{-1}(\hat{d}(\lambda_i, \lambda_j)) \tag{5}$$

and $u \equiv \hat{d}$ is the normalized distance. The distance function (d_{ij}) between any two points, λ_j and λ_i, on $\mathbf{\Omega}$ is given by,

$$d_{ij} = d(\lambda_i, \lambda_j) = \sqrt{(x_j - x_i)^2 + (y_j - y_i)^2} \tag{6}$$

Plots of the distance matrix $\mathbf{d}$ for a *circle* ($\mathbf{d}_{circle}$) and an *ellipse* ($\mathbf{d}_{ellipse}$) is shown in Fig. 2. For illustrative purposes, each plot is shown from two viewpoints; a side view and a top view. Because of the symmetry inherit in the shape of a *circle*, $\mathbf{d}_{circle}$ has the unique feature of having the only profile containing diagonal lines with constant values. As a *circle* is stretched in a given direction, $\mathbf{d}_{circle}$ looses its symmetry. Construction of $\mathbf{d}$ for many objects has verified the uniqueness of $\mathbf{d}$ for a given shape [11].

When parts of an object boundary are missing $\mathbf{d}$ will also change from its original profile. However, if the amount of boundary missing is relatively small then $\mathbf{d}$ will not change by much. This can be shown as follows: Let μ denote the percentage of boundary missing. Fig. 3 shows three variations of a *circle* with different amount of its original boundary missing along with their corresponding

d. We see that when the amount of boundary missing is small ($\mu = 0.1$) $\mathbf{d}_{circle\_0.9}$ is very similar to $\mathbf{d}_{circle}$. But as the amount of boundary missing increases the similarity of **d** to its original **d** decreases. But even when large amount of its boundary is missing, such as the case for the *circle* with 50% of its original boundary missing, we see that a large similarity exists between $\mathbf{d}_{circle\_0.5}$ and $\mathbf{d}_{circle}$ that the shape can be identified as being (part of) a *circle*. It is this similarity in **d** and the other boundary features presented that we exploit in our work to arrive at successful matching when partial boundary information is missing.

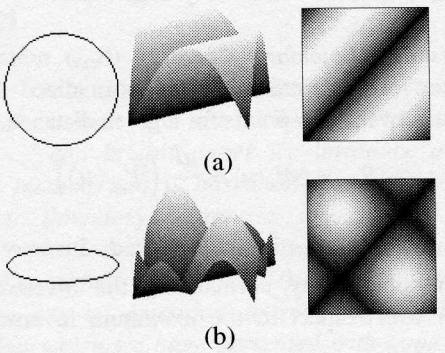

Fig. 2. Plots of **d**. (a) for a *circle*; $\mathbf{d}_{circle}$ and (b) an *ellipse* with eccentricity 0.995; $\mathbf{d}_{ellipse}$

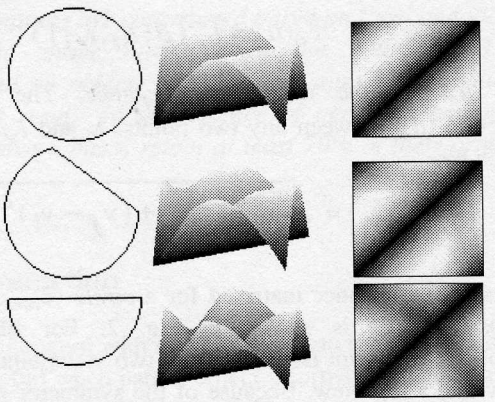

Fig. 3. Surface plots of the distance matrix (**d**) for a *circle* with different amount of its border missing (from top to bottom): $\mathbf{d}_{circle\_0.9}$ ($\mu = 0.1$), $\mathbf{d}_{circle\_0.7}$ ($\mu = 0.3$) and $\mathbf{d}_{circle\_0.5}$ ($\mu = 0.5$).

3.2 The Parameter Boundary Signature

The *Parameter Boundary Signature* ($\mathbf{S}_{PB}$) represents the frequency of occurrence of the chord bending between two points at a given value,

$$\mathbf{S}_{PB} = \mathrm{pdf}_{\gamma}(z) = \frac{d}{dz}\left(\tilde{\Psi}_{\gamma}(z)\right) \tag{7}$$

where $\tilde{\Psi}_{\gamma}$ denote the normalized inverse chord bending function obtained by normalizing the inverse chord bending function with respect to its maximum inverse chord bending value and $z \equiv \hat{\gamma}$ is the normalized chord bending function. Chord bending (γ), represents the amount of parameter bending between two points on $\mathbf{\Omega}$. For two points, $\lambda_i, \lambda_j \in \mathbf{\Omega}$, the chord bending is defined as the ratio of the distance function between the two points (d_{ij}) to the parameter distance between the two points (p_{ij}),

$$\gamma_{ij} = \gamma(\lambda_i, \lambda_j) = d_{ij} \,/\, p_{ij} \tag{8}$$

Since $\mathbf{\Omega}$ is closed, two different values of p exist between any pair of points, one in the counter-clockwise direction (p_{ij}^{+}) and the other in the clockwise direction (p_{ij}^{-}). The shortest of the two distances is taken as the parameter distance between the two points. Hence,

$$\gamma_{ij} = \frac{d_{ij}}{\min(p_{ij}^{+}, p_{ij}^{-})} \tag{9}$$

γ is symmetric. Note that if $\gamma_{ij} = 1$, then all points λ_k between $i \le k \le j$ lie on a straight line. Furthermore, the chord bending between any pair of successive points is unity, $\gamma_{i,i+1} = 1$. A plot of the chord bending matrix (γ) for a *circle* and an *ellipse* is shown in Fig. 4. The profile of an *ellipse* is distinctly different from that of a *circle*.

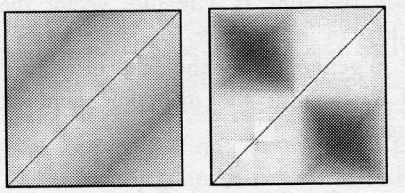

Fig. 4. Plot of the chord bending matrix (γ) for a *circle* (left) and an *ellipse* (right)

3.3 The Curvature Boundary Signature

The *Curvature* (or *Tangent) Boundary Signature* ($\mathbf{S}_{CB}$) represents the frequency of occurrence of the curvature for a point on $\mathbf{\Omega}$ at a given angle,

$$\mathbf{S}_{CB} = \mathrm{pdf}_{\kappa}(w) = \frac{d}{dw}\left(\tilde{\Psi}_{\kappa}(w)\right) \tag{10}$$

where $\tilde{\Psi}_\kappa$ denote the normalized inverse tangent angle function obtained by normalizing the inverse tangent angle function with respect to its maximum inverse tangent angle value and $w \equiv \kappa^\circ$ is the local curvature. The local curvature (κ°), represent the amount of local boundary bending by computing the local angle of the tangent, and is computed by,

$$\kappa_i^\circ = \cos^{-1}(\hat{\mathbf{v}}_{i-1} \cdot (-\hat{\mathbf{v}}_i)) \cdot \text{sign}(\hat{\mathbf{v}}_{i-1} \times \hat{\mathbf{v}}_i) \qquad (11)$$

where

$$\hat{\mathbf{v}}_i = \frac{\mathbf{v}_i}{|\mathbf{v}_i|} \qquad (12)$$

$$\mathbf{v}_i = r((x_{i+1} - x_i)\hat{\mathbf{i}} + (y_{i+1} - y_i)\hat{\mathbf{j}}) \qquad (13)$$

Values of κ° lie in the range $[0, 2\pi]$ where values of κ° between $0 < \kappa^\circ \leq \pi$ indicate shape concavities while values of κ° between $\pi < \kappa^\circ < 2\pi$ indicate shape convexities. Plots of κ° for a *circle* and an *ellipse* are shown in Fig. 5. We see that a *circle* has values of $\kappa^\circ = \pi$ everywhere. The profile of an *ellipse* is similar to that of a *circle*, but has smaller values of κ° at the ends of its major axis (dependent on eccentricity and profile resolution).

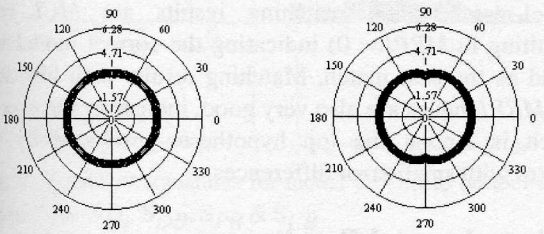

(a) (b)

Fig. 5. Polar plots for the values of κ° for (a) *circle* and (b) *ellipse* ($e = 0.995$).

3.4 The Angle Boundary Signature

The *Angle* (or *Direction*) *Boundary Signature* ($\mathbf{S}_{AB}$) represents the frequency of occurrence of two points oriented relative to each other at a certain angle and is given by,

$$\mathbf{S}_{AB} = \text{pdf}_\alpha(v) = \frac{d}{dv}\left(\tilde{\Psi}_\alpha(v)\right) \qquad (14)$$

where $\tilde{\Psi}_\alpha$ denotes the normalized inverse relative orientation function obtained by normalizing the inverse relative orientation function with respect to the maximum inverse relative orientation value and $v \equiv \alpha$. The relative orientation of point $\lambda_j = (x_j, y_j)$ with respect to λ_i, is given by,

$$\alpha(\lambda_i, \lambda_j) = \arctan^*(y_j - y_i,\ x_j - x_i) \qquad (15)$$

where λ_i and $\lambda_j \in \boldsymbol{\Omega}$. Values of α lie in the range $[0, 2\pi[$. Note that $\boldsymbol{\alpha}$ is skew symmetric, $\alpha_{ij} = -\alpha_{ji}$.

3.5 Discrete Boundary Signature Construction

Because of the discrete nature of images, obtaining an analytical expression for the signatures as stated above is not practical. The signatures we construct from images are the discrete counterpart of the analytical expressions stated above. If M_{DB} is the number of bins of $\mathbf{S}_{DB}$ with bin size $1/M_{DB}$, then the ith element of the signature is calculated by,

$$\mathbf{S}_{DB}^{<i>} = \tilde{\Psi}_d((i+1)/M_{DB}) - \tilde{\Psi}_d(i/M_{DB}) \qquad (16)$$

where $i = 0, 1, \ldots, M_{DB} - 1$. Similarly for the other signatures,

$$\mathbf{S}_{AB}^{<i>} = \tilde{\Psi}_\alpha((i+1)/M_{AB}) - \tilde{\Psi}_\alpha(i/M_{AB}) \qquad (17)$$

$$\mathbf{S}_{CB}^{<i>} = \tilde{\Psi}_\kappa((i+1)/M_{CB}) - \tilde{\Psi}_\kappa(i/M_{CB}) \qquad (18)$$

$$\mathbf{S}_{PB}^{<i>} = \tilde{\Psi}_\gamma((i+1)/M_{PB}) - \tilde{\Psi}_\gamma(i/M_{PB}) \qquad (19)$$

where M_{AB}, M_{CB} and M_{PB} are the number of bins of $\mathbf{S}_{AB}$, $\mathbf{S}_{CB}$ and $\mathbf{S}_{PB}$, respectively. In our work we employ signature sizes of $M_{DB} = 200$ for $\mathbf{S}_{DB}$ and $M_{PB} = 360$ for $\mathbf{S}_{PB}$. A signature bin size of $1/2\pi$ (i.e. 1°) is employed for $\mathbf{S}_{AB}$ and $\mathbf{S}_{CB}$ producing $M_{AB} = 360$ and $M_{AB} = 360$.

4. Matching

In this section an explanation of the signature matching strategy is explained as well as the indexes used to evaluate the matching performance.

4.1 Signature Matching

Matching between observed objects to model objects is accomplished by comparing their signatures using the four error metrics described in [3]. These metrics compare the signature profiles based on signature distance, variance, spread and correlation. The four error metrics are then

combined to form the *signature match error* (E), which gives a weighted signature error based on the four error metrics. We will refer to the correct model that an object should match to as the *model-match*. This paper will concentrate on evaluating the matching performance and missing data sensitivity of the four boundary signatures. Hence, the signature match error E will be calculated individually for each of the four boundary signatures (i.e. E_{AB}, E_{DB}, E_{PB} and E_{CB}) and evaluated. A small error value of E for a particular boundary signature indicates strong similarity between surfaces based on the boundary attribute.

4.2 Matching Performance

The following indexes are used to measure the performance of the signatures:

- **Relative Performance Index.** The *relative performance index* (*RPI*) is defined as the relative surface (object) match error of a model-surface (model-object) to an observed-surface (observed-object) with respect to all model-surface (model-object) errors in the model set. Hence, the *RPI* of a model-surface (model-object) indicates how well a model-surface (model-object) matched to an observed-surface (observed-object) with respect to other model-surfaces (model-object) in the set.
- **Model Percentile.** The *model percentile* (*CI*) is defined as the signature matching error percentile of matching model m to object o. A *CI* value of $n\%$ for a particular model indicates that $n\%$ of the models produced lower matching errors than this particular model.
- **Signature Recognition Rate and Recognition Efficiency.** The *signature recognition rate* (Φ) is defined as the percentage of correct hypotheses found for a given set using a particular signature type. The *signature recognition efficiency* (η) is define as the efficiency of a signature in matching a surface (object) to its model-match surface (object) for a given surface (object),

$$\eta = (1 - AMCI)\cdot 100\ \% \qquad (20)$$

where *AMCI* is the average model-match percentile of a set.

- **Surface (Object) Matching Performance Index of a Set.** The *surface (object) matching performance index –SMPI* (*OMPI*) is a measure of how well observed-surfaces (observed-objects) match to their model-match surfaces (objects), with respect to all model-surfaces (model-objects) in the set,

$$OMPI = (1 - AMRPI)\cdot 100\% \qquad (21)$$

where *AMRPI* is the average model-match's *RPI*.Values of *SMPI* (*OMPI*) lie in the range between [0%,100%]. A value close to 100% indicates that most of the observed-surfaces (observed-objects) match very well to their model-match, with respect to all model surfaces objects in the set.

4.3 Significance of Performance Metrics

The three metrics Φ, η and *SMPI* (*OMPI*) complement each other in measuring the signature matching performance for a given set of surfaces (objects). While Φ measures the percentage of surfaces (objects) that correctly produced a hypotheses, η measures the efficiency of matching by taking into consideration how "far off" -in terms of matching rank- the model-match is from the hypotheses found. *SMPI* (*OMPI*) measures how well the model-match matched -in terms of matching similarity- with respect to all models in the set. We will be interested primarily in the model-matchs' *CI* and *RPI* denoted by *MCI* and *MRPI*, respectively. While *MCI* indicates the rank of the model-match among the models, *MRPI* identifies the relative matching strength of the model-match. Ideal matching results are *MCI* = 0 (resulting in *MRPI* = 0) indicating the correct model was found as the best match. Matching results with low *MCI* and *MRPI* values are also very good, indicating the correct match is among the top hypotheses produced by the system with small error differences.

5. Experimental Results

Tests were conducted on objects of different shapes and sizes. The model set consisted of the 41 objects shown in Fig. 6. Shape signature files for these models were constructed off-line and stored in the model database. Boundary signatures for a sample model is shown in Fig. 7. Testing was done on two sets; The first set consisted of objects that completely visible while the second set consisted of objects that were partially visible.

5.1 Matching Complete Objects

Testing was done on 129 instances of the models at different scales and random rotations. In addition 6 instances of 2 new models not in the database were also tested to observe if the system can produce a hypothesis

which agrees with the closest model perceived visually. Several test images of the objects are shown in Fig. 8. Boundary signatures for these objects were constructed and subsequently matched to the signatures of the model database The results of matching are discussed in [12] and a summary follows:

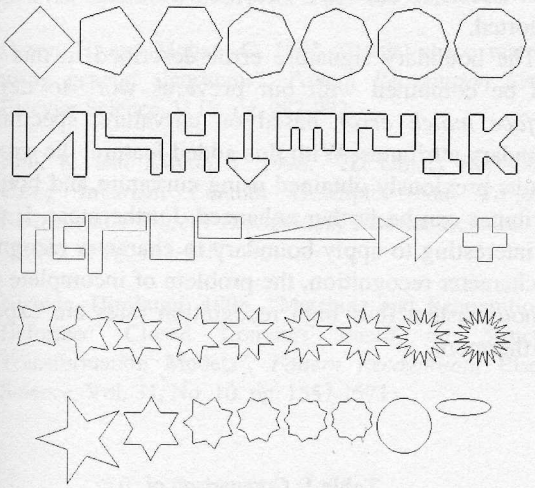

Fig. 6. Database models

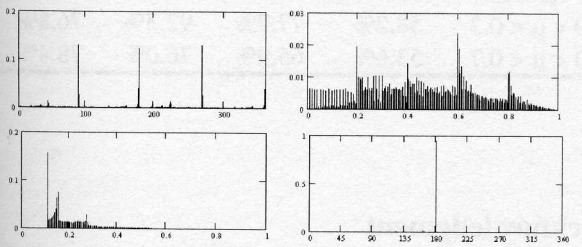

Fig. 7. Boundary signatures for model *C*. Top to bottom and left to right. $\mathbf{S}_{AB}$, $\mathbf{S}_{DB}$, $\mathbf{S}_{PB}$ & $\mathbf{S}_{CB}$

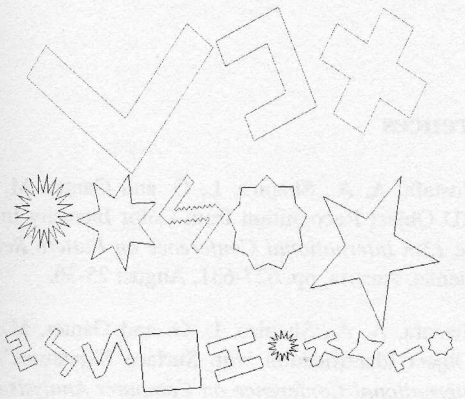

Fig. 8. Sample objects

- The combined results of $\mathbf{S}_{DB}$ and $\mathbf{S}_{PB}$ correctly detected 129 of 135 objects ($\Phi_{DB \cup PB} = 95.6\%$).
- The signature efficiency using $\mathbf{S}_{DB}$ and $\mathbf{S}_{PB}$ are very high ($\eta_{DB} = 99.1\%$ and $\eta_{PB} = 91.1\%$, respectively). This indicates that using $\mathbf{S}_{DB}$ produced -on average- the model-match as the best match or the next best match, with a higher tendency for the former. The signature efficiency using $\mathbf{S}_{AB}$ and $\mathbf{S}_{PB}$ are very poor ($\eta < 60\%$).
- Matching using $\mathbf{S}_{DB}$ produced the best signature matching success rate where 124 of the 135 objects were correctly hypothesized ($\Phi_{DB} = 91.9\%$). Matching using $\mathbf{S}_{PB}$ produced the second best matching rate ($\Phi_{PB} = 63.7\%$). Matching using $\mathbf{S}_{CB}$ produced poor matching results ($\Phi_{CB} = 15.6\%$) while matching using $\mathbf{S}_{AB}$ produced the poorest matching results ($\Phi_{AB} = 8.1\%$).

5.2 Matching Incomplete Objects

In this section we present the results of matching incomplete objects. The amount of data missing will be measured as the percentage of original boundary missing and will be denoted by μ. Tests on incomplete objects consisted of 70 objects. μ varied for these objects from $\mu = 0.12$ to $\mu = 0.61$ with an average value of $\mu = 0.37$. Fig. 9 shows a sample of these shapes. Matching results for these objects in the complete range tested were as follows:

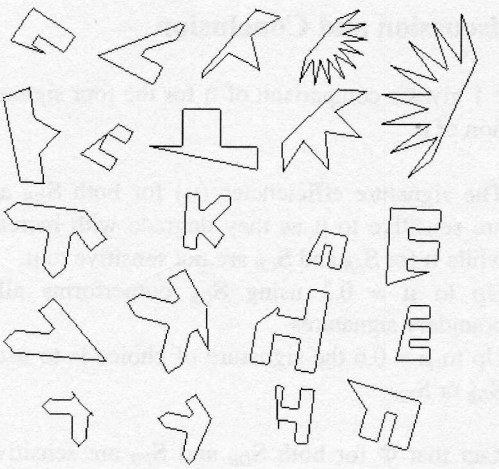

Fig. 9. A sample of the incomplete objects

- The overall success rate of the signatures were all very weak, where $\Phi < 20\%$ for all four signatures. Matching using S_{DB} produced the highest success rate ($\Phi_{DB} = 19.5\%$) followed by S_{CB} ($\Phi_{PB} = 14.6\%$). Matching using either S_{AB} or S_{PB} produced the poorest results ($\Phi_{AB} = 2.4\%$ and $\Phi_{PB} = 7.3\%$).
- However, the signature efficiencies varied from $\eta = 53.6\%$ to $\eta = 78.4\%$. S_{PB} had the best performance with $\eta_{PB} = 78.4\%$ followed by S_{DB} with $\eta_{DB} = 76.0\%$. S_{CB} and S_{AB} both had poor performances with $\eta = 65.9\%$ and $\eta = 53.6\%$, respectively.

However, analyzing the results for $\mu < 0.3$ (**70% boundary retention**) we find that:

- The performance of S_{DB} and S_{CB} are much better: $\Phi_{DB,\mu<0.3} = 66.7\%$ and $\Phi_{PB.,\mu<0.3} = 16.6\%$.
- The signature efficiencies for both S_{DB} and S_{CB} improve considerably: $\eta_{DB} = 92.3\%$ and $\eta_{CB} = 77.7\%$.

From the points mentioned above, it is obvious that a correlation exists between μ and *MCI* for S_{DB} and S_{PB}. The correlation coefficient calculated for the four signatures are 0.110, 0.764, 0.647 and 0.120 for S_{AB}, S_{DB}, S_{PB} and S_{CB}, respectively. These correlation coefficients indicate, as earlier observed, that a strong correlation exists between the amount of boundary missing and the model-match percentile for S_{DB} and S_{PB}, and no correlation exists between the amount of boundary missing and the model-match percentile for S_{AB} and S_{CB}.

6. Discussion and Conclusion

Table 1 gives a comparison of η for the four signatures as function of μ.

- The signature efficiencies (η) for both S_{DB} and S_{PB} are sensitive to μ as they degrade with increasing μ while η for S_{AB} and S_{CB} are not sensitive to μ.
- Up to $\mu = 0.3$ using S_{DB} outperforms all other boundary signatures.
- Up to $\mu = 0.6$ the signature of choice is to use either S_{DB} or S_{PB}.

The fact that Φ for both S_{DB} and S_{PB} are sensitive to μ while S_{DB} and S_{PB} are not is due to the fact that the former pair of signatures are dependent on the distance between boundary points. When an object is partially visible and incomplete, the object takes on a new shape defined by the boundary of its visible part resulting in an object boundary with smaller inter-distances between its boundary points. As the amount of the boundary missing (μ) increases the distortion in distance increases. On the other hand, S_{CB} is a function of the boundary curvature which retains its correct values on the visible boundary. S_{AB} is a function of the inter-direction between boundary points and as long as only a non-significant part of the object is missing the inter-direction between boundary points is not greatly distorted.

The boundary signature error described in this paper can be combined with our previous work to define a *surface match error* based on curvature, spectral and boundary attributes. With this added feature, the excellent results previously obtained using curvature and boundary attributes can be further enhanced. Furthermore, It would be interesting to apply boundary to character recognition. In character recognition, the problem of incomplete shape is non-existent thus high recognition rates are expected. Furthermore,

Table 1: Comparison of η

μ	S_{AB}	S_{CB}	S_{DB}	S_{PB}
$\mu = 0$	52.8%	59.9%	99.1%	91.1%
$0 < \mu < 0.3$	58.2%	77.7%	92.3%	76.8%
$0 < \mu < 0.7$	53.6%	65.9%	76.0%	78.4%

Acknowledgment

The author would like to thank the Kuwait University Research Administration for providing financial support for this research through KU-Grant EM-112.

References

[1] Mustafa, A. A., Shapiro, L. G. and Ganter, M. A. 1996. "3D Object Recognition from Color Intensity Images". In the *13th International Conference on Pattern Recognition*, Vienna, Austria, pp. 627-631, August 25-30.

[2] Mustafa, A. A., Shapiro, L. G. and Ganter, M. A. 1997. "Object Identification with Surface Signatures". The *7th International Conference on Computer Analysis of Images And Patterns*, Kiel, Germany, pp. 58-65, Sept. 10-12.

[3] Mustafa, A. A., Shapiro, L. G. and Ganter, M. A. 1999. "3D Object Identification with Color and Curvature Signatures". *Pattern Recognition*, Elsevier Science. Vol. 32, No. 3, pg. 1-17.

[4] Hong, D., Sarkodie-Gyan, T., Campbell, A. and Yan, Y. 1998. "A Prototype Indexing Approach To 2-D Object Description And Recognition". *Pattern Recognition*, Elsevier Science. Vol. 31, No. 6, pg. 699-725.

[5] Ozcan, E. and Mohan, C. 1997. "Partial shape matching using genetic algorithms". *Pattern Recognition Letters*, Elsevier Science .V 18, pg. 987-992.

[6] Roh, K. and Kweon, I. 1998. "2D Object Recognition Using Invariant Contour Descriptor And Projective Refinement". *Pattern Recognition*, Elsevier Science. Vol. 31, No. 4, pg. 441-455.

[7] Nishida, Hirobumi. 1998. "Matching and Recognition of Deformed Closed Contours Based on Structural Transformation Models", *Pattern Recognition*, Elsevier Science. Vol. 31, No. 10, pg. 1557-1571.

[8] Mokhtarian, F., Abbasi, S. and Kittler, J. 1996. "Robust and Efficient shape Indexing through Curvature Scale Space". In the *British Machine Vision Conference*, Edinburgh. pg. 53-62.

[9] Kovalev, V. and Petrou, M. 1996. "Multidimensional Co-occurrence Matrices for Object Recognition and Matching", *GMIP*, V58 (3), pp. 187-197.

[10] Loncaric, Sven 1998. "A survey of shape analysis techniques". *Pattern Recognition*, Elsevier Science .Vol. 31, No. 8, pg. 983-1001.

[11] Mustafa, A. A. "Object Matching using Surface Boundary Signatures". Kuwait University, Dept. of Mechanical Engineering, Tecchnical Report #EMM-112, Sept. 1999.

[12] Mustafa, A. A. "Object Matching using Shape Surface Signatures". *SPIE conference on Machine Vision Applications in Industrial Inspection IX*, San Jose, Ca., Jan 22-23, 2001.